MINGHUI MA, Ph.D.[1]
E-mail: maminghui1989@hotmail.com
SHIDONG LIANG, Ph.D.[2]
(Corresponding author)
E-mail: sdliang@hotmail.com
HU ZHANG, Ph.D.[2]
E-mail: zhhoo11@163.com
[1] School of Mechanical and Automobile Engineering
Shanghai University of Engineering Science
Shanghai, 201620, China
[2] Department of Transportation Systems Engineering
University of Shanghai for Science and Technology
Shanghai, 200093, China

A DYNAMIC COMPETITION CONTROL STRATEGY FOR FREEWAY MERGING REGION BALANCING INDIVIDUAL BEHAVIOUR AND TRAFFIC EFFICIENCY

ABSTRACT

An integrated control strategy is considered in this paper with the aim of solving congestion in freeway merging regions during peak hours. Merging regions discussed in this paper include the mainline and on-ramp. Traditional research mainly focuses on the efficiency of traffic, ignoring the experience of on-ramp drivers and passengers. Accordingly, a dynamic competition control strategy is proposed to balance individual behaviour and traffic efficiency. First, the concept of the congestion index is introduced, which is expressed by the queue length and the speed parameter of the merging region. The congestion index is used to balance the priorities of the vehicles from the mainline and on-ramp into the merging region in order to avoid poor individual behaviour of on-ramp drivers due to the long-time waiting. Additionally, a nonlinear optimal control approach integrating variable speed limits control and ramp metering is proposed to minimize the total time spent and the maximum traffic flow. The integrated control approach proposed in this paper is tested by simulation which is calibrated using field data. The results indicate that the integrated control approach can effectively shorten the total delay and enhance the traffic service level.

KEY WORDS

transportation; intelligent transportation systems; variable speed limits; traffic control strategy; ramp metering;

1. INTRODUCTION

Congestion in freeway networks has been recognized as a common issue. In general, the issue of traffic congestion can be solved by changing linear structure of the road or adopting traffic management measures. However, the structure of the road changed, such as building a new traffic infrastructure or expanding the road capacity, requires a lot of labour power, material resources, and money. To seek a better way to relieve congestion in freeway networks, a large number of control approaches have been developed and improved over the last few decades, such as the freeway mainline control, on-ramp control, and corridor control. Traffic congestion in a merging region of a freeway network is one of the major topics in the domain of transportation. In general, this problem can be solved in two different ways based on the characteristics of the merging region traffic: (1) control of the outflow of the on-ramp; (2) restriction of the traffic flow of the upstream mainline of the merging region.

Some studies indicated that a reasonable speed limit on freeway can improve transport service quality [1, 2]. The Variable Speed Limits (VSL) control, as a popular mainline traffic control approach, is applied widely in the field of transportation. This approach is proposed and developed as a practically useful tool to improve the traffic service level of the mainline. The efficiency of the VSL control in terms of improving traffic safety and traffic order has been proved by digital and dynamic simulations [3-7]. The key control parameter of the VSL control is the traffic speed which can be obtained using a set of methods, such as optimal, adaptive, and intelligent methods. At present, popular VSL control strategies can be categorized as those that (a)

emphasize the homogenization of traffic speeds [8-10]; (b) focus on the prevention of freeway traffic breakdown [11, 12]; and (c) limit the flows in the control region [13]. Although such VSL control approaches can improve the quality of service, applying VSL control to the upstream mainline of the merging region only is insufficient to get reliable results when congestion occurs in the ramp merging region [14].

To address this issue, by considering the characteristics of the traffic congestion in the merging region, the mainline VSL control and on-ramp metering are integrated over a finite horizon, e.g. one peak period. The merging region is assumed in this paper to consist of the mainline and on-ramp. The congestion in the merging region stems from the confluence of the outflows of the upstream mainline and on-ramp. Ramp metering is an effective approach to limit the number of on-ramp vehicles flowing into the merging region [15]. In previous studies, ramp metering involved two different policies, the static threshold strategy and the dynamic response strategy [16-20]. The metering rate of the static threshold strategy is a set of fixed values which are computed based on the historical traffic data and environmental characteristics. The scope of the static threshold strategy is limited to simply managing the on-ramp traffic when the demand is low and presents certain regularity. However, the on-ramp traffic may show several fluctuation changes in response to the traffic demand of the freeway network. In this paper, the case is considered when the traffic demand is high in the merging region. Accordingly, the dynamic response strategy is selected as the on-ramp metering approach. The dynamic response strategy mainly restricts the outflow of the on-ramp dynamically based on the real-time traffic data. It is shown that the integrated control, involving VSL control and ramp metering, can effectively prevent traffic breakdowns in the merging regions [21, 22]. A series of approaches integrating VSL control and freeway metering were proposed by constructing nonlinear constrained optimal control methods [23]. Although previous works proved the efficiency of the integrated control method [24-26], they ignored several important issues, such as how to balance the priority between mainline traffic and ramp traffic in the freeway merging region. Generally, when traffic congestion appears in the merging region, the on-ramp vehicles flowing into the merging region are limited until there is enough space in

the merging region [27]. However, on-ramp vehicles have to wait for too long when the demand is high. Therefore, poor experience of the drivers on the ramp should be taken into consideration. This paper aims to develop an overarching framework to solve this difficult problem.

This paper analyses previous studies and presents a new strategy to integrate VSL control and ramp metering considering an innovative dynamic competition control strategy. More specifically, the congestion index is the key parameter of the dynamic competition control strategy, which is included to ensure the priority of on-ramp and mainline vehicles. It is well known that the queue and the speed can well describe the variation of the traffic flows in a freeway network. Therefore, the queue and the speed parameters are selected as the basis of the congestion index. The main contributions are presented as follows:

- A dynamic competition control strategy is considered in this paper, which can balance the relationship between individual behaviour and traffic efficiency in the merging region of freeway networks.
- Queue, as a significant parameter of the principle of distribution of rights, is derived based on the nonlinear macroscopic traffic flow model.
- A nonlinear optimal control approach, integrating the mainline Variable Speed Limits control and on-ramp control, is proposed through the derivation of the model with the consideration of the dynamic competition control strategy.

This paper is organized as follows. Section 2 defines the macroscopic traffic flow model and its extensions. Section 3 describes the characteristics of congestion in the merging region. In Section 4, a novel dynamic competition control strategy is proposed to manage the right of roads. The designed control strategy and sufficient optimality conditions are discussed in Section 5. Section 6 presents three case studies based on a simple network. The main conclusions are summarized in Section 7.

2. TRAFFIC FLOW MODEL

The METANET presents the sharpness of an expounded dynamic expression of traffic behaviour. The deduction process of the METANET is shown in [28]. The relevant parameters are described as follows. First, the basic mainline link m is selected randomly. According to the METANET, link m should be divided into N_m segments of length Δl_m which is

the product of the discrete time interval Δt (typically, $\Delta t = 10s$) and the free-flow speed $v_{f,m}$. In segment $N_{i\in(1,2,...,N_m)}$, during the discrete-time instant $t=k\Delta t$ ($k=0,1,...,k_p$), where k_p is the time frame, the average number of vehicles on each kilometre of road space is denoted as traffic density $\rho_{m,i}(k)$. The number and the average speed of vehicles flowing into segment N_i are denoted as $q_{m,i}(k)$ and $v_{m,i}(k)$, respectively. The $\rho_{cr,m}$ and $\rho_{c,m}$ represent the critical density and the capacity of link m, respectively.

The VSL control is implemented in this paper to restrict upstream vehicles in the merging region. Accordingly, the macroscopic traffic flow model is extended to describe the traffic variables under VSL control in the merging region. The classical METANET model describes the fundamental relationships among the macroscopic traffic parameters of the freeway network. VSL control is adopted in this paper as a popular mainline control approach. The traffic conditions may exhibit several unusual changes under VSL control compared to conditions without control. For example, when VSL control is applied to the freeway mainline, the VSL values shown in the Variable Message Sign (VMS) should decrease with a corresponding increase in the traffic demand. The VSL values are implemented instead of legal limit values to restrict the arrival rate of the mainline vehicles.

In the free-flow scenario, the upper limit of the dynamic speed limit value is equivalent to the legal speed limit. The desired traffic speed under VSL control is equivalent to the free-flow speed without control. In the congestion scenario, with the VSL instead of the legal speed limit, the drivers are restricted by the VSL values. The desired speed is equal to a fixed value between the VSL value and the self-organized speed. Furthermore, in the jam scenario, all vehicles on the roads must follow the self-organized operation. Therefore, the desired speed $V_{m,i}[\rho_{m,i}(k)]$ under the VSL control is given by

$$V_{m,i}[\rho_{m,i}(k)] =$$
$$= \min\left(v_{f,m}\exp\left[-\frac{1}{\alpha_m}\left(\frac{\rho_{m,i}(k)}{\rho_{cr,m}}\right)^{\alpha_m}\right], \\ \eta v_{vsl,m,i}(k) + (1-\eta)v_{f,m}\exp\left[-\frac{1}{\alpha_m}\left(\frac{\rho_{m,i}(k)}{\rho_{cr,m}}\right)^{\alpha_m}\right]\right) \quad (1)$$

where $v_{vsl,m,i}(k)$ is the speed limit value of segment i of link m; α_m expresses a nonlinear relationship between the traffic density and speed, which can be obtained by the data fitting results; and η is the adjustment parameter indicating whether drivers obey the VSL control [27]. Especially, if $\eta=1$, the drivers obey the VSL values completely; if $\eta=0$, no drivers follow the VSL values; otherwise, when $0<\eta<1$, a part of drivers obey the VSL values. According to the basic METANET and *Equation 1*, the description about the traffic operation under the VSL control can be completed.

3. PROBLEM FORMULATION

The outflow of the merging region is restricted by the traffic capacity of the merging region and the demand of the upstream mainline and on-ramp traffic. The basic road characteristics are illustrated in *Figure 1*. During the peak period several disturbances will occur in the merging region with the intertwinement of the mainline and on-ramp flows. This paper mainly focuses on the traffic condition of the merging region. In order to develop the optimal control model, the basic traffic characteristics of the merging region should be defined by a traffic flow model. Compared to the mainline region, the traffic characteristics of the merging region are more complex. This assumes an ideal scenario with no traffic accidents or lane drops in the merging region.

In *Figure 2*, two different shapes of the Fundamental Diagram (FD) show significant changes between the formulation concept and the real-world scenario. Note that the traffic capacity is achieved when the density reaches critical value ρ_k. In *Figure 2*, ρ_k^e and ρ_J^e are the traffic critical density and jam density
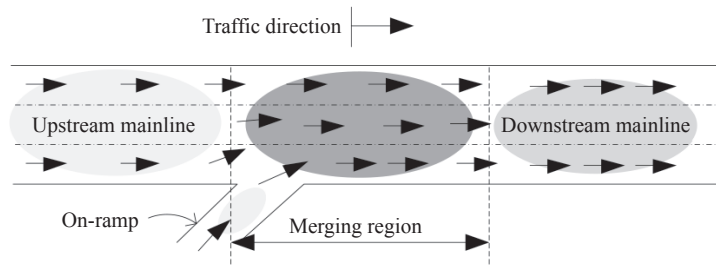

Figure 1 – Merging region of a freeway network
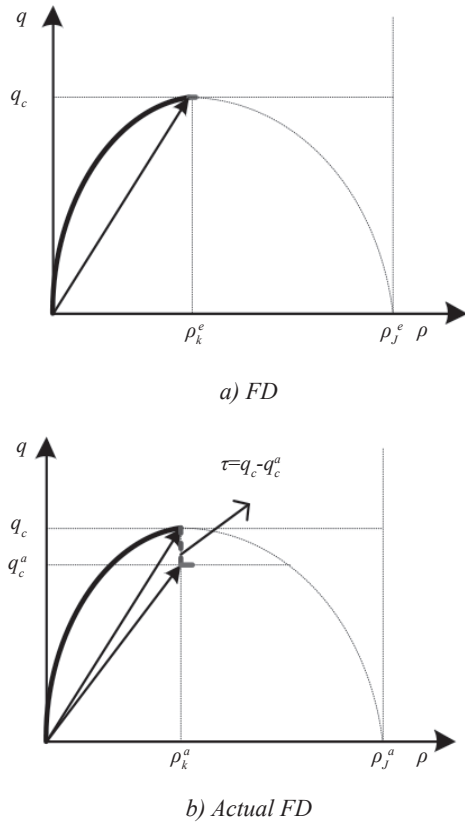
a) FD

b) Actual FD

Figure 2 – Different shapes of the fundamental diagram

under the ideal condition, respectively; and ρ_k^a and ρ_J^a are the traffic critical density and jam density under the real condition, respectively. A theoretical traffic condition change can be defined by the relationship between the traffic demand and density, shown in *Figure 2a*. In *Figure 2a*, it can be seen that the traffic flow is always at a high level, which is an ideal fundamental diagram. In practice, there are a lot of disturbance factors in vehicle operation, such as traffic lane changing behaviour. *Figure 2b* shows the approximate FD based on the real-world condition. The comparison of *Figures 2a* and *2b* can provide an insight regarding significant differences. In *Figure 2b*, a decline in the capacity is shown when the critical density is reached. The decline is $\tau=q_c-q_c^a$, where q_c and q_c^a are the capacity under the ideal condition and

the real condition, respectively. Previous studies have described the decrease in capacity in specific scenarios [29-31]. The maximum traffic flow is an important index to evaluate the traffic service level.

A traffic node is defined as a traffic distribution point, which is used for transmitting vehicles from the upstream link to downstream links. In order to ensure the integrity constraint, a sample scenario is used to support the description of traffic parameters in the merging region. Note that this paper only focuses on the common merging region with one on-ramp and mainline.

In *Figure 3*, there are two mainline links (link m and link $m+1$) and one on-ramp r_m. The traffic direction is from left to right. In addition, the traffic volume flowing into link $m+1$ $q_{in,m+1}(k)$ can be expressed as a function of both $q_{in,m}(k)$ and $q_{r_m}(k)$, which is shown as

$$q_{in,m+1}(k) = q_{out,m}(k) + q_{r_m}(k) \tag{2}$$

Notably, when the traffic demand is higher than the capacity of the merging region ($q_{in,m+1}(k) \geq q_{c,m+1}$), a traffic breakdown in the merging region of the freeway network occurs based on the former description. The maximum outflow from link m $q_{out,m}(k)$ can be expressed as the minimum flow between the last segment of link m and the capacity of link m $q_{c,m}$.

$$q_{out,m}(k) = \min\{v_{m,N_m}(k)\rho_{m,N_m}(k)\lambda_m, q_{c,m}\} \tag{3}$$

where $v_{m,N_m}(k)$ and $\rho_{m,N_m}(k)$ are the traffic average speed and density in the last segment N_m of link m, respectively; and λ_m is the number of the line in link m.

Similarly, the outflow of on-ramp $q_{r_m}(k)$ can be described as

$$q_{r_m}(k) = \min\{\rho_{r_m,N_{r_m}}(k), v_{r_m,N_{r_m}}(k)\lambda_{r_m}, q_{c,r_m}\} \tag{4}$$

where $\rho_{r_m,N_{r_m}}(k)$ and $v_{r_m,N_{r_m}}(k)$ are the traffic average density and speed in the last segment N_{r_m} of on-ramp r_m; and q_{c,r_m} is the capacity of on-ramp r_m.
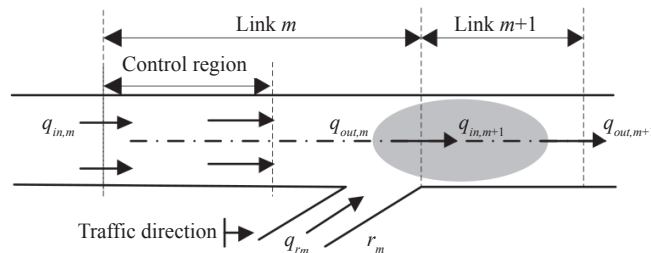

Figure 3 – Freeway segments in a merging region

The constraint condition of the outflow of the merging region is given as follows to understand the composition of the traffic flow. Specifically, the traffic demand of both upstream mainline and on-ramp should be restricted by the capacity of the merging region $q_{c,m+1}$. The necessary constraint is presented as

$$\max\{q_{out,m}(k) + q_{rm}(k)\} \leq q_{c,m+1} \tag{5}$$

The specifics of the merging region (including the on-ramp) demand that the conservation equation of the METANET should be replaced by the following equation:

$$\rho_{mB,i}(k) = \rho_{m,i}(k-1) + \\ + \frac{\Delta t}{L_m \lambda_m}[q_{m,i-1}(k-1) - q_{m,i}(k-1) + q_{rmN_{rm}}(k)] \tag{6}$$

Taking into account the mainstream traffic speed decrease caused by on-ramp traffic flowing into the merging region, the adjustment coefficient becomes

$$-\frac{\delta \Delta t q_0(k) v_{m,1}(k)}{L_m \lambda_m (\rho_{m,1}(k) + \kappa)} \tag{7}$$

where δ is defined as a constant parameter, which is computed based on the field data; $q_0(k)$ is the traffic flow coming from the upstream of link m; $v_{m,1}(k)$ is the traffic speed of the first segment of link m; κ is global constant parameter which is achieved by a series of parameters (such as traffic environment and vehicles condition), which is used for depicting the characteristic of the traffic system.

4. COMPETITION CONTROL STRATEGY

4.1 Basic idea

This paper mainly focuses on the equilibrium of the outflow of the upstream mainline and on-ramp under the precondition of maximizing the outflow of the merging region. The merging region is called

a dangerous region due to the special road lines and traffic perturbations (frequent deceleration, acceleration, lane-changing, etc.). With an increase in the traffic demand, the traffic problem of the merging region becomes more serious. Therefore, a reasonable control approach should be proposed for seeking the optimal traffic environment. Though there is plenty of literature on how to solve the merging region congestion, most of these methods give priority to the upstream mainline vehicles flowing into the merging region. Especially during the peak period, it may lead to a long queue of on-ramp vehicles that may induce traffic spill-back. Accordingly, this paper proposes a competition strategy addressing this issue.

Specifically, the queue as a response variable can describe the congestion condition [32-34]. If there are queues on both mainline and on-ramp, the priority to the longest queue should be given. However, if there are no queues on the mainline and on-ramp, the control strategy based on the queue parameter would fail. An auxiliary parameter evaluating the traffic condition should be provided in this scenario. Speed is an important characteristic describing the traffic state in the absence of queues. This paper focuses on a merging region that includes a mainline and on-ramp. Since speeds are different on the mainline and on-ramp, the rates of speed change are adopted as auxiliary parameters.

4.2 Competition strategy

A traffic network is considered as a directed graph which consists of links connecting a set of nodes. The used notation is presented in *Figure 4*. In detail, the nodes are the connection points between the mainline and ramp or between mainline and mainline. With the difference of node types caused by a series of influential factors (road environment,
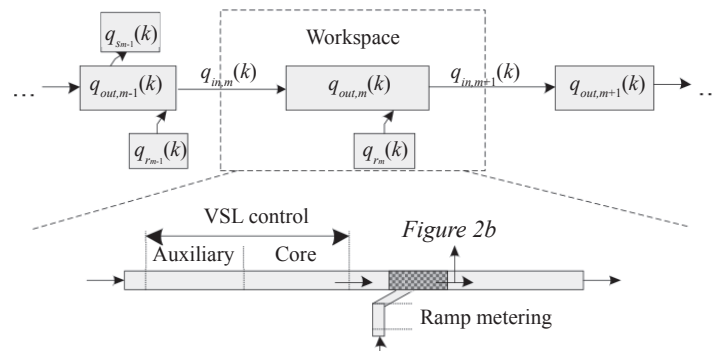

Figure 4 – Regional architecture decomposition

driving demand, economic factors, etc.), the length of link in traffic network is different. The tested mainline considered in this paper is long enough and the traffic congestion in the merging region does not have an impact on other merging regions or diverging areas. There are two main control regions: one is the VSL control region and the other is the on-ramp metering region. Specifically, the VSL control region is divided into two parts which are the auxiliary area and the VSL control region depending on the road characteristics. The auxiliary area, as the auxiliary region of the VSL control region, mainly helps to enhance the effects of VSL control by slowly reducing the speed. The auxiliary area length can be obtained by the number of the speed intervals shown in the variable message sign and the length between each variable message sign.

Basically, the queue on the tested road and the speed variation in the last segment are adopted as the evaluated parameters. It is assumed that the queue and speed in each link are given. If there are queues in the merging region (including the upstream mainline and on-ramp), the congestion evaluation indices based on the dynamic queue are mathematically represented as

$$\varphi_m^q(k) = \frac{w_m(k)}{L_{m,D}} \ \& \ \varphi_{r_m}^q(k) = \frac{w_{r_m}(k)}{L_{r_m,D}} \tag{8}$$

where $\varphi_m^q(k)$ and $\varphi_{r_m}^q(k)$ are the evaluation indices based on the queue on the mainline and on-ramp, respectively; $w_m(k)$ and $w_{r_m}(k)$ are the queues calculated as in Remark 1; and $L_{m,D}$ and $L_{r_m,D}$ are the lengths of the adjustment regions.

Another evaluation index adopted in this paper is the speed variation $\varphi_{m/r_m}^v(k)$, which can be defined as

$$\varphi_m^v(k) = \frac{v_{f,m} - v_{m,N_m}(k)}{v_{f,m}} \ \& \ \varphi_{r_m}^v(k) = \frac{v_{f,r_m} - v_{r_m,N_{r_m}}(k)}{v_{f,r_m}} \tag{9}$$

where $v_{m,N_m}(k)$ and $v_{r_m,N_{r_m}}(k)$ are the average speeds of vehicles in the last segment of the upstream mainline and on-ramp, respectively.

The homogenization parameters are calculated by Equation 10.

$$\beta^q = \begin{cases} \beta_m^q(k) = \dfrac{\varphi_m^q(k)}{\varphi_m^q(k) + \varphi_{r_m}^q(k)} \\[2mm] \beta_{r_m}^q(k) = \dfrac{\varphi_{r_m}^q(k)}{\varphi_m^q(k) + \varphi_{r_m}^q(k)} \end{cases}$$

$$\&$$

$$\beta^q = \begin{cases} \beta_m^v(k) = \dfrac{\varphi_m^v(k)}{\varphi_m^v(k) + \varphi_{r_m}^v(k)} \\[2mm] \beta_{r_m}^v(k) = \dfrac{\varphi_{r_m}^v(k)}{\varphi_m^v(k) + \varphi_{r_m}^v(k)} \end{cases} \tag{10}$$

The outflow of the merging region may be restricted by the condition of the merging region and the demand of the upstream mainline and on-ramp. The homogenization parameters β^q and β^v have an important effect on the control parameters of the mainline and on-ramp. Specifically, the outflow of the merging region is lower than its capacity with the traffic disturbance in the merging region. Accordingly, the outflow is expressed by Equation 11.

$$q_{out,m}(k) = \min\{\omega_m \rho_{m,N_m}(k)\lambda_m, q_{c,m}, q_{c,m+1}, v_{m,N_m}(k)\rho_{m,N_m}(k)\lambda_m\} \tag{11}$$

where ω_m is the competition parameter which can be expressed as $\omega_m = \vartheta\beta_m^q(k) + (1-\vartheta)\beta_{r_m}^v(k)$. Further, ϑ obeys the 0-1 distribution. If there is a queue in the upstream mainline or on-ramp, ϑ is equal to 1; otherwise, ϑ is equal to 0. Similarly, the outflow of on-ramp r_m is given by Equation 12.

$$q_{r_m}(k) = \min \begin{cases} \omega_{r_m} \rho_{r_m,N_{r_m}}(k)v_{r_m,N_{r_m}}\lambda_{r_m}, q_{c,r_m} \\ q_{c,m+1} - \min\{v_{m,N_m}(k), v_{N_m,vsl}(k)\}\rho_{m,N_m}(k)\lambda_m \end{cases} \tag{12}$$

where the competition parameter ω_{r_m} is given by $\omega_{r_m} = \vartheta\beta_{r_m}(k) + (1-\vartheta)\beta_m^v(k)$.

4.3 A simple case study

In order to present the working principle of the competition parameter, a simple case study is shown as follows. In this simple case study conducted, more attention is paid to the outflows and the queue length on the mainline and on-ramp.

First, it is assumed that the values of the mainline and on-ramp line are 1,000 veh. and 500 veh., respectively, while the initial values of the queue length are 800 veh. and 100 veh. The total inflow to the mainline and ramp is 10 veh./min, while the total outflow is the same as the inflow, and the proportions for ramp and mainline are random. This can ensure that the total queue length of the on-ramp and mainline is stable. In addition, in this simple case study, only the queue length is considered as the evaluation index, which is more visual to understand the working principle of the evaluation index. Based on the setting mentioned above, the evolution of the queue length and the outflow for both ramp and mainline can be presented as in Figure 5.

Figure 5 presents the queue length evolution, the evaluation index fluctuation and the outflow for both mainline and ramp. As shown in Figure 5a, at the beginning the queue length on the mainline decreased greatly from 800 veh. to 600 veh., while
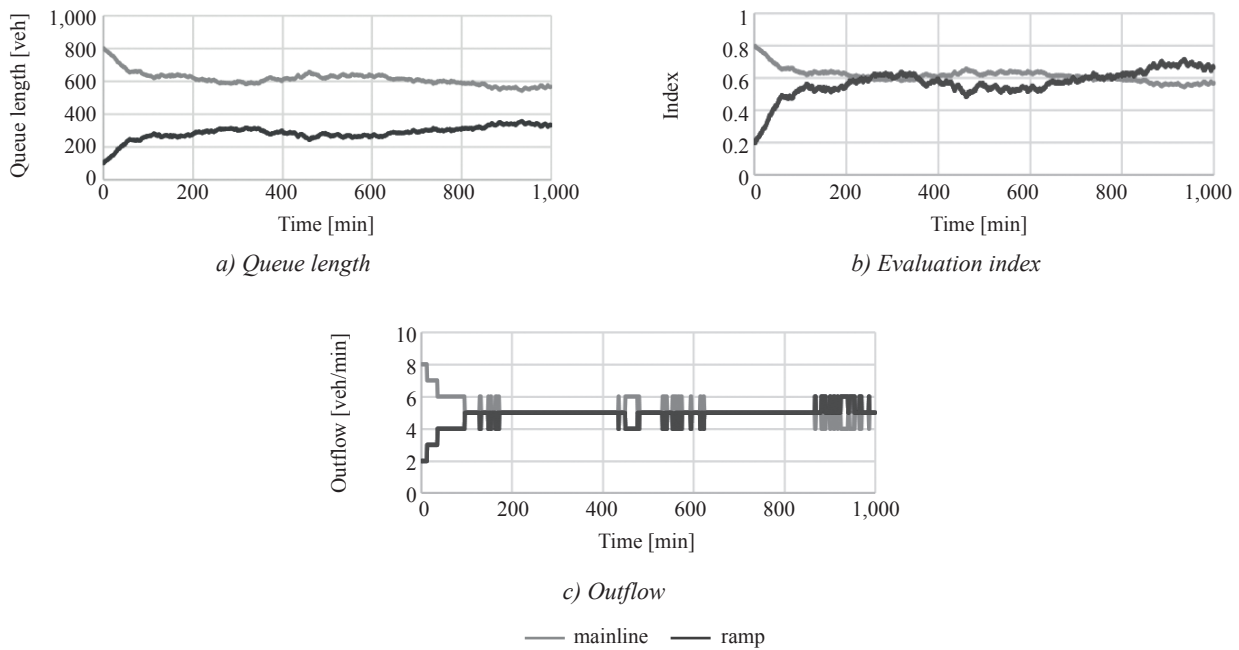
a) Queue length

b) Evaluation index

c) Outflow

—— mainline —— ramp

Figure 5 – Queue length evolution under the effect of evaluation index

the queue length on the ramp increased greatly from 100 veh. to 300 veh.. More insight reason for this change can be obtained from *Figure 5b*. At the beginning, the initial evaluation indices of mainline and ramp are 0.8 and 0.2, respectively, which means the traffic condition of the mainline is more congested. When the time is about 100 min, the evaluation indices for both mainline and on-ramp are around 0.6, which means the congestion degree of the mainline and on-ramp becomes the same. Theoretically, the evaluation indices for the mainline and on-ramp should both be equalized to 0.6, and the queue length of the mainline is 600 veh. while the queue length of on-ramp is 300 veh., whose total queue length is 900 veh. equalized with the total initial queue length 900 veh. (800 veh. + 100 veh.). Since the inflow is random, the value of the competition parameter cannot be stable. Comparing *Figures 5b* and *5c*, the relationship between the evaluation indices and the outflows of the mainline and on-ramp can be obtained. During two periods, from 0 min to 200 min, and from 440 min to 620 min, the outflow of the mainline is larger than the one of the on-ramp, because the competition parameter of the mainline is larger than the one of the on-ramp. On the contrary, during the period from 870 min to 1,000 min, the outflow of the on-ramp is larger than the one of the mainline, because the competition parameter of on-ramp is larger. Therefore, according to this simple case study, the competition parameter reflecting

the congested degree can balance the outflow of the mainline and on-ramp making maximum use of the freeway network.

Remark 1. The explicit solution of the dynamic queue estimation problem is given as follows.

The queue, as the basic traffic parameter to construct the competition strategy, has to be obtained precisely. Although numerous studies and modifications of the queue estimation have been proposed, there are a lot of parameters used in these methods that need to be calibrated. To address the issue, at the same time keeping the convenience of the control approach and the accuracy of the queue estimation, a simple but effective method is presented to describe the dynamic queue based on the density in each segment. Essentially, the queue parameters can be obtained in two steps including the queue tail segment recognition and the queue length measurement. Note that if there is a queue on the tested road, the queue tail cell cannot provide enough space to accept all vehicles coming from the upstream segment.

First, a simple queue tail segment recognition framework is described in *Figure 6*. The density in each segment is selected as the key parameter to approximately determine the queue tail position. Specifically, if the density of segment i $\rho(k)$ is greater than the density of segment i-1 $\rho_{i-1}(k)$ and less than the density of segment i+1 $\rho_{i+1}(k)$ ($\rho_{i+1}(k) \geq \rho_{dc}$), the queue tail is located in segment i-1 or segment i.

Furthermore, if the number of vehicles flowing into segment i $q_i(k)T$ is less than or equal to the number of vehicles in segment i-1 $\lambda_{i-1}L_{i-1}\rho_{i-1}(k-1)$, the queue tail is located in segment i-1; otherwise, the queue tail is located in segment i. Note that the critical density ρ_{dc} is a dynamic parameter.
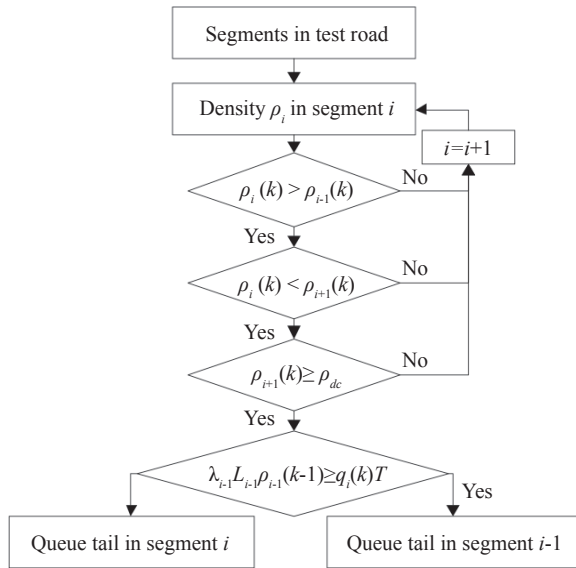

Figure 6 – The queue tail segment recognition framework

According to *Figure 6*, the queue tail location can be approximately determined. To get the accurate position of the queue tail further, it is necessary to try to determine the segment structure based on the density parameter. The queue tail segment is shown in *Figure 7*. In order to describe the calculation of the queue length easily, it is assumed that the queue tail is located in segment i.
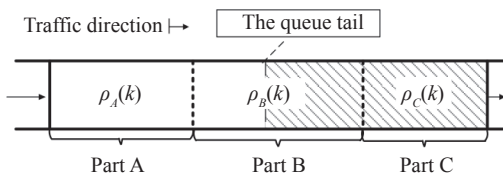

Figure 7 – Density in the queue tail segment

Figure 7 shows that the queue tail segment is divided into three parts based on the density separation, including Part A, Part B, and Part C. In this paper, the queue tail is defined as the terminal position where the shockwave propagates, so that the queue can be estimated based on the density of the three parts. First, it is assumed that the queue tail is

located in Part B. The traffic condition in Part A is similar to the upstream traffic segment. Therefore, the density of Part A $\rho_A(k)$ is approximately equal to the density of the upstream segment i-1. If the queue length is longer than the length of Part C, the density in Part C $\rho_C(k)$ is approximately equal to the density of segment i+1 $\rho_{i+1}(k)$. In Part B, the volatility of the traffic parameter is reflected in the density $\rho_B(k)$. According to the former assumption, all vehicles in Part C belong to the queue. Note that the critical density of the dynamic queue is higher than the density of Part A, and lower than the density of Part C. Therefore, there is a tiny subsection in which the density is equal to the critical density in Part B. In addition, for the convenience of calculation, the queue tail segment i is divided into two dynamic regions, which is depicted in *Figure 8*. *Equation 13* presents several relations among parameters, which is a basic set of formulas.
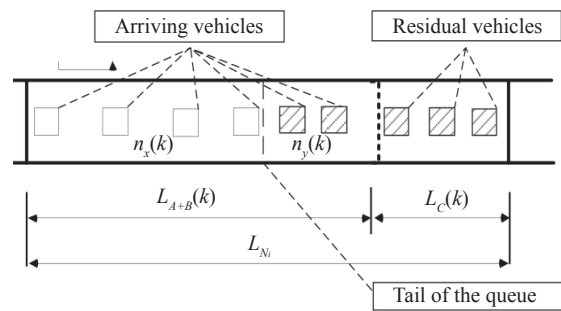

Figure 8 – Vehicle distribution in the queue tail segment

$$\begin{cases} L_{A+B}(k) = \dfrac{n_x(k)}{\rho_A(k)\lambda_i} + \dfrac{2n_y(k)}{\rho_A(k)\lambda_i + \rho_C(k)\lambda_i} \\ n_x(k) + n_y(k) = \rho_i(k)\lambda_i L_{N_i} - \rho_C(k)\lambda_i L_C(k) \\ \rho_A(k) = \rho_{i-1}(k) \\ \rho_C(k) = \rho_{i+1}(k) \end{cases} \quad (13)$$

where $n_x(k)$ is the number of vehicles in Part A and $n_y(k)$ is the number of vehicles in Part B.

According to *Equation 13*, the number of vehicles in Part A and Part B can be expressed as *Equation 14*.

$$\begin{cases} n_x(k) = \dfrac{\left(\begin{array}{l} L_{A+B}(k)\rho_A(k)\lambda_i(\rho_A(k)+\rho_C(k))- \\ 2(\rho_i(k)L_{N_i} - \rho_C(k)L_c(k)) \end{array}\right)}{(\rho_C(k) - \rho_A(k))} \\ \\ n_y(k) = \dfrac{\left(\begin{array}{l} (\rho_i(k)L_{N_i} - \rho_C(k)L_c(k))(\rho_C(k)-\rho_A(k))- \\ L_{A+B}(k)\rho_A(k)\lambda_i(\rho_A(k)+\rho_C(k))- \\ 2(\rho_i(k)L_{N_i} - \rho_C(k)L_c(k)) \end{array}\right)}{(\rho_C(k) - \rho_A(k))} \end{cases} \quad (14)$$

where $L_{A+B}(k)=L_i - L_c(k)$ and

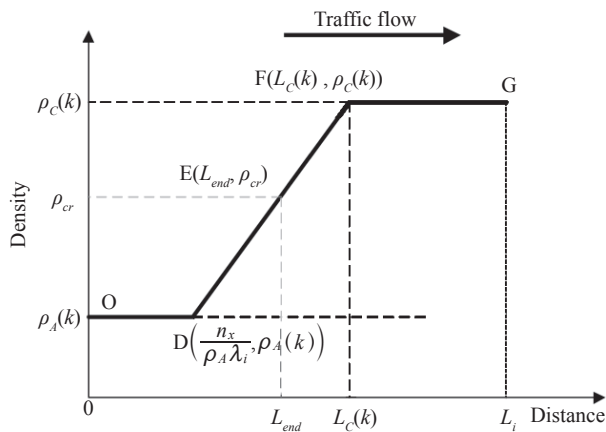$$L_c(k) = \frac{\rho_i(k-1)L_i\lambda_i - q_{i+1}(k-1)\Delta t}{\rho_C(k)\lambda_i}.$$

Figure 9 – Density distribution in the queue tail segment

In order to calculate the queue length accurately, it is assumed that the density of Part B changes linearly from $\rho_A(k)$ to $\rho_C(k)$ as shown in *Figure 9*.

In *Figure 9*, point E is the location of the queue tail; line OD is the density of Part A; and line FG is the density of Part C. The queue length $L_{end}(k)$ in the queue tail segment can be calculated by simple trigonometry formulas as *Equation 15*.

$$L_{end}(k) = \frac{2\lambda_i \cdot n_y \cdot \rho_A(k) \cdot (\rho_c - \rho_A(k)) + \lambda_i \cdot n_x \cdot (\rho_c^2(k) - \rho_A^2(k))}{\rho_A(k) \cdot (\rho_c^2(k) - \rho_A^2(k))} \quad (15)$$

The total queue length $w(k)$ on the tested road can be calculated as the cumulative length of the downstream tail segment and $L_{end}(k)$.

$$w(k) = \sum_{f=i+1}^{N_{m/rm}} L_f + \frac{2\lambda_i \cdot n_y \cdot \rho_A(k) \cdot (\rho_c - \rho_A(k)) + \lambda_i \cdot n_x \cdot (\rho_c^2(k) - \rho_A^2(k))}{\rho_A(k) \cdot (\rho_c^2(k) - \rho_A^2(k))} \quad (16)$$

5. OPTIMIZATION PROBLEM FORMULATION

The main component of the integrated optimization control approach includes the mainline, the VSL control and the ramp metering. The integrated control approach is proposed as discrete-time dynamic control over a given optimization horizon k_p. The state variables include the speed and density, and the control variables include the mainline VSL value and the metering rate.

The purpose of this paper is to propose methodological strategies specific to the integrated control method to balance the control goals including the Total Time Spent (*TTS*) and the Total Traffic Flow

(*TTF*). The minimum of the Total Time Spent and the maximum of the Total Traffic Flow are the main goals of the integrated optimization control. The Total Time Spent is the sum of the time which vehicles spend on the mainline and the waiting time on the on-ramp. The function can be described as

$$\min TTS = \Delta t \sum_{k=1}^{k_p} \left[\sum_{i=1}^{N_m} \lambda_{m,i} L_{m,i} \rho_{m,i}(k) + \sum_{j=1}^{N_{rm}} \lambda_{rm,j} L_{rm,j} \rho_{rm,j}(k) \right] \quad (17)$$

The inflows of the freeway merging region consist of two parts, the upstream mainline flow and the on-ramp flow. Accordingly, the Total Traffic Flow function can be defined by

$$\max TTF = \Delta t \left[\begin{array}{l} \sum_{k=1}^{k_p} \lambda_m \rho_{m,N_m}(k) v_{vsl}(k_{control}) + \\ \sum_{k=1}^{k_p} \lambda_{rm} \rho_{rm,N_{rm}}(k) v_{rm,N_{rm}}(k) r_{rm}(k_{control}) \end{array} \right] \quad (18)$$

where $\rho_{r_m N_{r_m}}(k)$ and $\rho_{m,N_m}(k)$ are the densities of segment N_{r_m} and segment N_m, respectively.

The controller is to optimize the whole control system over the test horizon by balancing the former two goals. Therefore, the optimal function can be described as:

$$\min J = \alpha_S \Delta t \sum_{k=1}^{k_p} \left[\sum_{i=1}^{N_m} \lambda_{m,i} L_{m,i} \rho_{m,i}(k) + \sum_{j=1}^{N_{rm}} \lambda_{rm,j} L_{rm,j} \rho_{rm,j}(k) \right] - \alpha_F \Delta t \left[\sum_{k=1}^{k_p} \lambda_m \rho_{m,N_m}(k) v_{vsl}(k_{control}) + \sum_{k=1}^{k_p} \lambda_{rm} \rho_{rm,N_{rm}}(k) v_{rm,N_{rm}}(k) r_{rm}(k_{control}) \right] \quad (19)$$

where α_T and α_F are the correlation coefficients calculated for the *TTS* and *TTF*. Specifically, the basic traffic parameters follow the macroscopic traffic flow model considered in this paper. The control variable of on-ramp $r_{r_m}(k_{control})$ lies in [0, 1]. The variable speed limit value $v_{vsl}(k_{control})$ changes from 0 to the speed of the freeway mainline V_d (this speed is given in accordance with the actual conditions).

6. CASE STUDY

In order to illustrate the efficiency of the dynamic competition control strategy, three control strategies are covered in Section 6.1. Examples of the three control scenarios and the results are described in Section 6.2, Section 6.3, and Section 6.4.

6.1 Test plan description

In order to obtain the assessment results of the control approach, the congestion scenario in the merging region is considered. The tested road has a simple structure shown in *Figure 3*. To

illustrate the efficiency and suitability of the integrated control approach proposed in this paper, different control methods are applied to the same scenario through repeated experiments. Specifically, three control scenarios applied include the no-control (NC) scenario, the mainline VSL control (MC) scenario, and the integrated control (IC) scenario. First, the NC scenario is taken as the basic case where the traffic is limited by the legal speed. Second, the MC scenario is considered where the mainline control approach is realized in the upstream of the merging region. Third, the IC scenario is studied using the optimal control approach proposed in this paper.

Field data coming from Shanghai, China, are used to calibrate the related model parameters. The duration of each simulation is 2.5 hours, where the first 30 minutes are the warm-up period and the other 2 hours are used to make sure that the simulation can be evaluated. The length of the on-ramp in the tested freeway is one kilometre. The VSL control region is approximately 0.5 kilometres away from the merging region. The time interval Δt is 10 seconds, and the control time interval is 90 seconds. The legal speed limits in the mainline and on-ramp are 100 km/h and 40 km/h, respectively.

6.2 NC scenario

This section studies the no-control scenario and analyses the reason of congestion in the merging region of the test network. The results of the simulation experiment are shown in *Figure 10*. Vehicles on the test network are self-organized in the NC simulation system. There is enough space in the merging region to dynamically hold the outflow from the upstream mainline and on-ramp until 0.45 h. With an increase in the merging region traffic demand, the traffic structure exhibits an imbalance phenomenon between the traffic demand and the traffic supply.

At around 0.54 h, a traffic breakdown occurs in the merging region of the test network. The results show a dramatic decline, as shown in *Figure 10c*, which is similar to the results found in [35]. Queues on the upstream mainline and on-ramp are induced by the shock coming from the traffic congestion in the merging region. It is well known that vehicles in the freeway mainline have priority to enter the merging region. Therefore, the on-ramp queue forms earlier than the upstream mainline one, which can be seen in *Figures 10d* and *10e*. The maximum queue lengths on the upstream mainline and on-ramp are 1,183 metres and 767 metres, respectively.
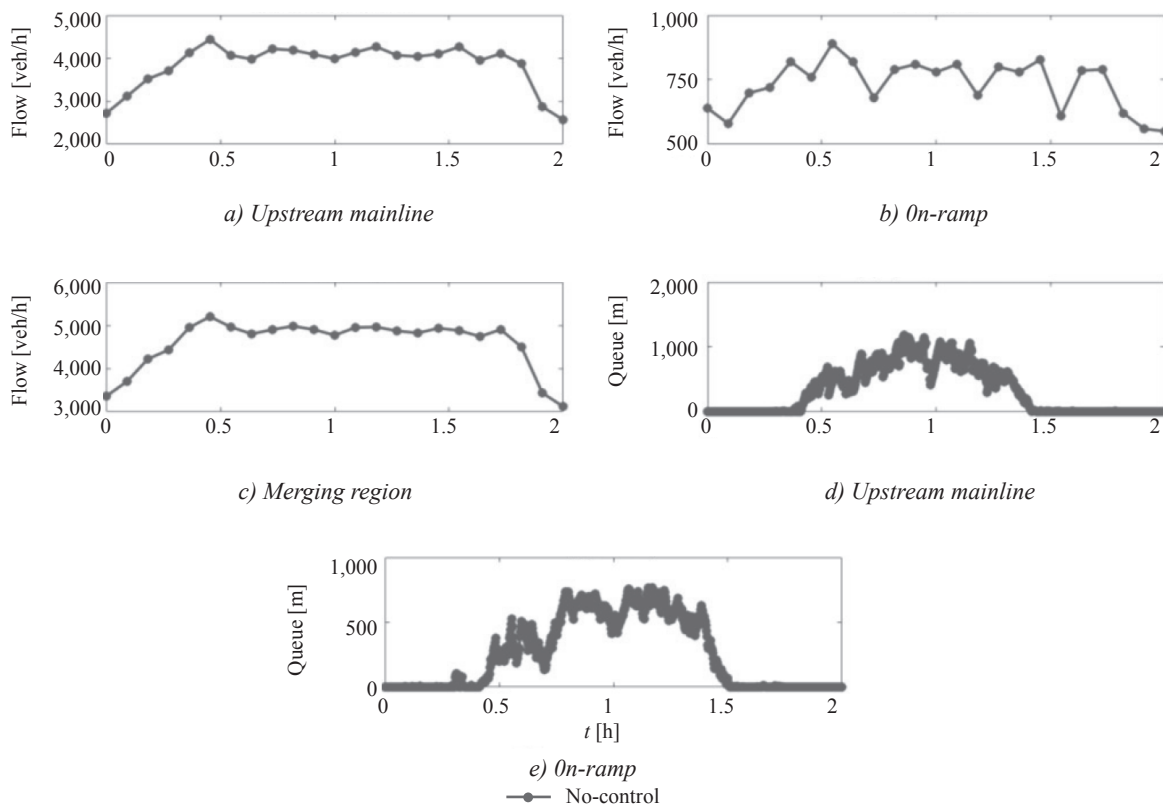

a) Upstream mainline

b) 0n-ramp

c) Merging region

d) Upstream mainline

e) 0n-ramp

— No-control

Figure 10 – NC scenario

6.3 MC scenario

In the MC scenario, the VSL control is applied to control the mainline vehicles and there is no control on the on-ramp. Particularly, the outflow of the upstream mainline is restricted by the VSL values. The vehicles on the on-ramp are self-organizing operation. The traffic parameter changes in the MC scenario are depicted in *Figure 11*. *Figure 12* presents the evolution of the VSL values (measured in km/h) over the iterations of the algorithm.

Figure 11 shows the traffic flows and queues on the tested road. Note a similar phenomenon of the traffic flow that has dropped during the simulated period in *Figure 11c*. Compared to the NC scenario, longer queues are formed in the upstream mainline of the merging region during the peak period. The maximum queue and the average queue on the upstream mainline reach 423 and 1,497 metres separately. The reason is that a series of lower mainline VSL values are adopted to restrict the inflow of the merging region. Ideally, there would be no queue on the on-ramp when the outflow of the upstream mainline is restricted. However, the intermittent queue on the on-ramp is depicted in *Figure 11e*, due to traffic disturbances in the merging region.
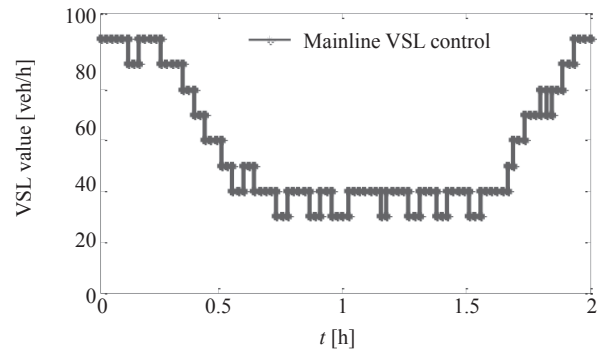

Figure 12 – VSL values

Therefore, based on the queue condition in NC and MC scenarios, the average queue on the on-ramp has a marked improvement under mainline control. Compared to the NC scenario, the average delay of on-ramp vehicles is reduced approximately by 64% in the MC scenario.

6.4 IC scenario

In the IC scenario, the dynamic competition control strategy and the integrated control approach are applied to relieve congestion in the merging region and to improve the efficiency of the test network.
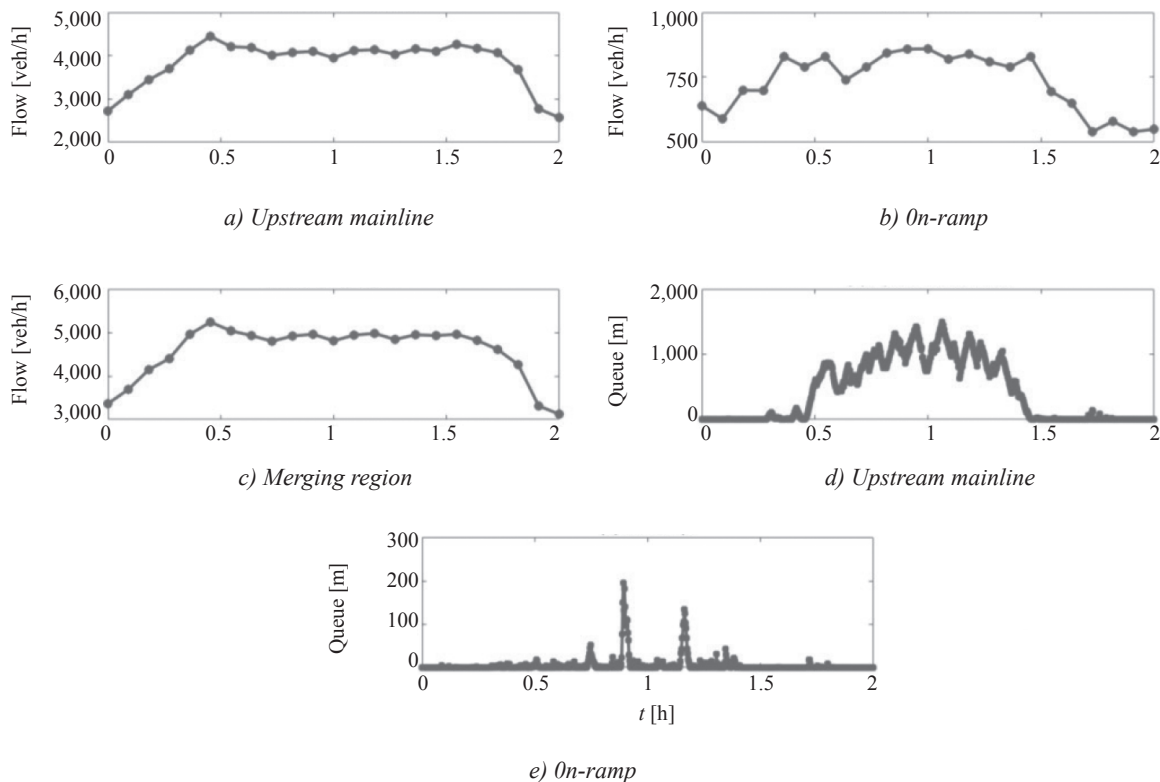

a) Upstream mainline

b) On-ramp

c) Merging region

d) Upstream mainline

e) On-ramp

— Mainline VSL control

Figure 11 – MC scenario

a) Upstream mainline

b) 0n-ramp

c) Merging region

d) Upstream mainline
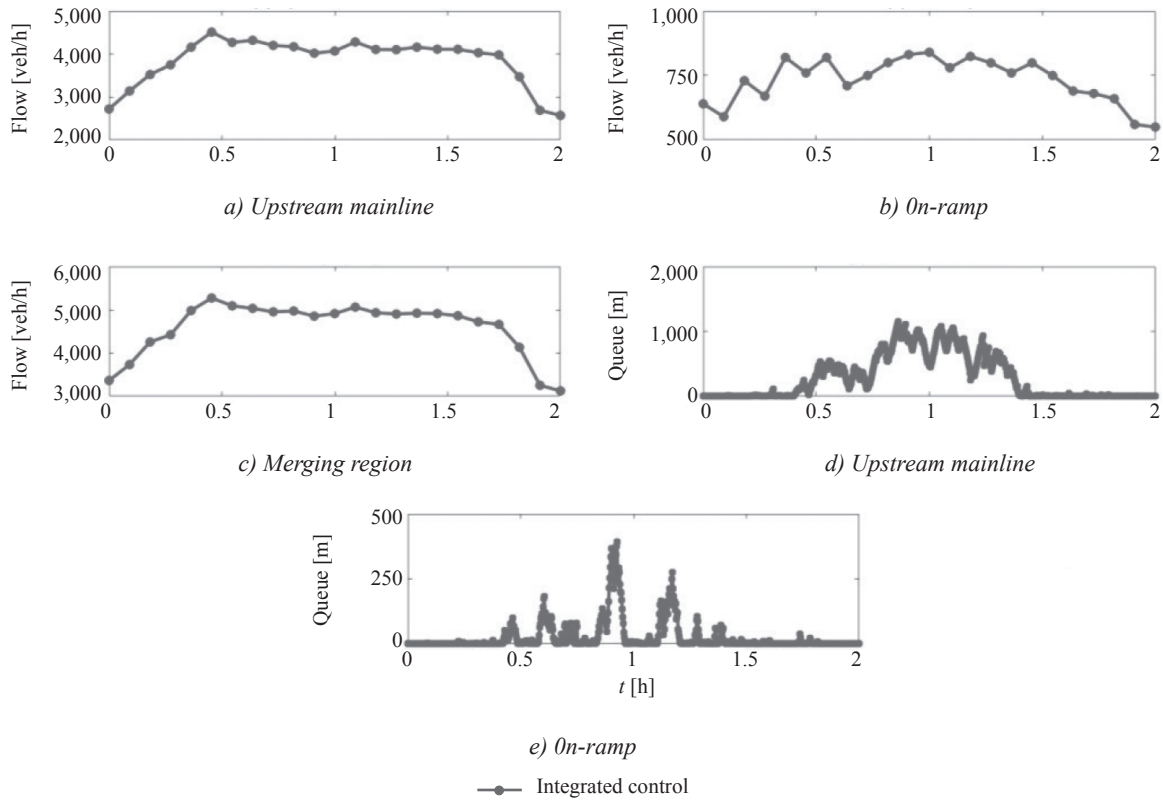

e) 0n-ramp

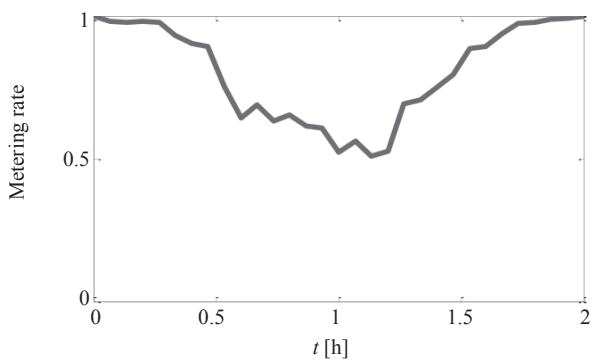Integrated control

Figure 13 – IC scenario
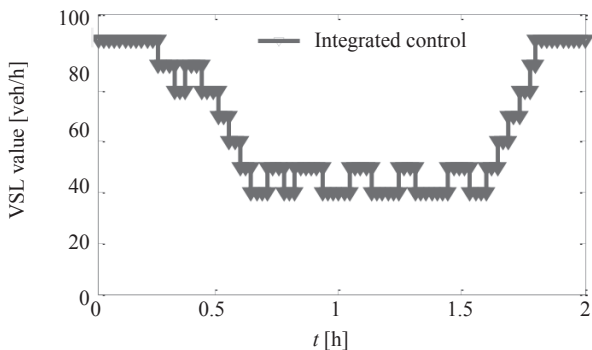

Figure 14 – Metering rates

Figure 15 – VSL values

The results are presented in *Figure 13*. *Figures 14* and *15* show the trajectories of the control variables including the on-ramp metering rates and VSL values.

During the peak period, a similar phenomenon of a sudden decline in the outflow of the merging region is illustrated in *Figure 13c*. By comparing the outflows of the merging region in the NC, MC, and IC scenarios, it can be seen that the outflow from the merging region in IC scenario has been cut, but by much less than under NC scenario and MC scenario during the peak period. The foremost reason is that the outflows of the upstream mainline and on-ramp are limited by the optimal control approach. As the demand increases, the performance of the IC becomes more remarkable. In order to relieve the congestion in the merging region and adjust the priority of vehicles in the test network, a series of the on-ramp rates and VSL values are calculated based on the optimal control approach considering the dynamic competition control strategy.

Figures 13d and *13e* display the trajectories of the queue on the upstream mainline and on-ramp. During the peak period, the maximum lengths of the upstream mainline queue and on-ramp reach 1,152 metres and 393 metres, respectively. The average queue on the upstream mainline reaches 277 metres lower than the one in both the NC and MC scenario. In addition, the average queue on the on-ramp is 157 metres, which is lower than that in the NC scenario and longer than that in the MC

scenario. The main reason is that the dynamic competition control strategy is applied in the IC scenario. In the same tested time period, more vehicles are served in the test network. Further, in the IC scenario, the improvements in the delay are approximately 23% and 14% compared to the NC and MC scenarios, respectively, which can be seen in *Table 1*. More precisely, IC improves the throughput of the merging region and the efficiency of the simulated network.

Table 1 – Comparison of performance indices

Scenarios	Average delay time [s/veh]	Improvement of delay [%]	Improved value [s/veh]
NC	87.80	22.75	19.97
MC	79.08	14.23	8.72
IC	67.83		

7. CONCLUSION

To enhance the traffic efficiency of the merging region in a freeway network, this paper proposes an integrated control strategy by considering a division of priority flows in both the mainline and on-ramp. By analysing the traffic parameter characteristics of the merging region, the queue length and the average speed were selected as the key parameters to construct a competition parameter for the evaluation of congestion on the tested road. A simple case study was considered to evaluate the efficiency of the dynamic competition control strategy proposed. To illuminate the improvement of the traffic quality, three control scenarios were designed. The results showed that the integrated control proposed can bring some advantage, such as enhancing the outflow from the merging region, improving the traffic congestion, and balancing the distribution of mainline and on-ramp vehicles. Besides, the results showed that the delay could be significantly reduced in IC scenario, which seems to be popular with drivers. In the future, more complicated control strategy will be considered in combination with the area control algorithm, such as traffic guidance. Linkages of influences among the merging regions in freeway network will be also studied in the following work.

马明辉，梁士栋，张虎

考虑个体感受和交通效率均衡的高速公路合流区动态竞争控制策略

摘要

本文考虑采用一种融合控制策略，旨在解决高速公路主线和匝道合流区交通拥挤问题。传统交通控制方法主要关注于如何提升交通效率，而忽略了匝道车辆驾驶员和乘客的个体感受。因此，本文提出一种动态竞争控制策略来平衡个体感受和交通效率。首先，交通拥挤指数概念被提出，其可通过合流区车辆排队长度和速度参数综合表达，主要用于确定匝道合流区主线和匝道车辆通行权，以防止匝道车辆等待时间过长而产生不良的通行感受。以此为基础，以总时间花费最小和通行交通量最大为目标，提出了一种融合主线可变限速控制和匝道控制的交通优化控制方法。采用实测数据对控制模型相关参数校准，并采用仿真手段进行实验验证。实验结果表明，该融合控制方法能够有效的缩短总交通延误，提升交通服务水平。

关键词
交通工程；智能交通系统；可变速度限制；交通控制策略；匝道控制

REFERENCES

[1] Zovak G, Kos G, Huzjan B. The Driver Behaviour and Impact of Speed on Road Safety on the Motorways in Croatia. *Promet – Traffic&Transportation*. 2017;29(2): 155-164. Available from: doi:10.7307/ptt.v29i2.2071

[2] Ziolkowski R. Effectiveness of Automatic Section Speed Control System Operating on National Roads in Poland. *Promet – Traffic&Transportation*. 2019;31(4): 435-442. Available from: doi:10.7307/ptt.v31i4.3060

[3] Smulders S. Control of freeway traffic flow by variable speed signs. *Transportation Research Part B: Methodological*. 1990;24(2): 111-132. Available from: doi:10.1016/0191-2615(90)90023-R

[4] Hegyi A, De Schutter B, Hellendoorn J. Optimal coordination of variable speed limits to suppress shock waves. *Transportation Research Record*. 2003;1852(1): 167-174. Available from: doi:10.3141/1852-21

[5] Hadiuzzaman M, Fang J, Luo Y, et al. Evaluating performance of a proactive optimal variable speed limit control using different objective functions. *Procedia-Social*

and Behavioral Sciences. 2013;96: 2895-2906. Available from: doi:10.1016/j.sbspro.2013.08.321

[6] Li Z, Li Y, Liu P, et al. Development of a variable speed limit strategy to reduce secondary collision risks during inclement weathers. *Accident Analysis & Prevention*. 2014;72: 134-145. Available from: doi:10.1016/j.aap.2014.06.018

[7] Wang W, Cheng Z. Variable speed limit signs: control and setting locations in freeway work zones. *Journal of Advanced Transportation*. 2017; 2017. Available from: doi:10.1155/2017/4390630

[8] Kejun L, Meiping Y, Jianlong Z, et al. Model predictive control for variable speed limit in freeway work zone. *2008 27th Chinese Control Conference*. IEEE; 2008. p. 488-493.

[9] Heydecker B G, Addison J D. Analysis and modelling of traffic flow under variable speed limits. *Transportation Research Part C: Emerging Technologies*. 2011; 19(2): 206-217. Available from: doi.org/10.1016/j.trc.2010.05.008

[10] Müller ER, Carlson RC, Kraus W, et al. Microsimulation analysis of practical aspects of traffic control with variable speed limits. *IEEE Transactions on Intelligent Transportation Systems*. 2015;16(1): 512-523. Available from: doi:10.1109/TITS.2014.2374167

[11] Nissan A, Koutsopoulosb HN. Evaluation of the impact of advisory variable speed limits on motorway capacity and level of service. *Procedia-Social and Behavioral Sciences*. 2011;16: 100-109. Available from: doi:10.1016/j.sbspro.2011.04.433

[12] Zhao X, Xu W, Ma J, et al. Effects of connected vehicle-based variable speed limit under different foggy conditions based on simulated driving. *Accident Analysis & Prevention*. 2019;128: 206-216. Available from: doi:10.1016/j.aap.2019.04.020

[13] Soriguera F, Martínez I, Sala M, et al. Effects of low speed limits on freeway traffic flow. *Transportation Research Part C: Emerging Technologies*. 2017;77: 257-274. Available from: doi:10.1016/j.trc.2017.01.024

[14] Ma M, Yang Q, Liang S, et al. A New Coordinated Control Method on the Intersection of Traffic Region. *Discrete Dynamics in Nature and Society*. 2016;2016. Available from: doi:10.1155/2016/5985840

[15] Abuamer IM, Celikoglu HB. Local ramp metering strategy ALINEA: Microscopic simulation based evaluation study on Istanbul freeways. *Transportation Research Procedia*. 2017;22: 598-606. Available from: doi:10.1016/j.trpro.2017.03.050

[16] Hourdakis J, Michalopoulos PG. Evaluation of ramp control effectiveness in two twin cities freeways. *Transportation Research Record*. 2002;1811(1): 21-29. Available from: doi:10.3141/1811-03

[17] Kotsialos A, Papageorgiou M. Efficiency and equity properties of freeway network-wide ramp metering with AMOC. *Transportation Research Part C: Emerging Technologies*. 2004;12(6): 401-420. Available from: doi:10.1016/j.trc.2004.07.016

[18] Khoo HL. Dynamic penalty function approach for ramp metering with equity constraints. *Journal of King Saud University-Science*. 2011;23(3): 273-279. Available

from: doi:10.1016/j.jksus.2010.12.004

[19] Yousif S, Al-Obaedi J. Modeling factors influencing the capacity of motorway merge sections controlled by ramp metering. *Procedia-Social and Behavioral Sciences*. 2011;16: 172-183. Available from: doi:10.1016/j.sbspro.2011.04.440

[20] Tian Q, Huang H-J, Yang H, et al. Efficiency and equity of ramp control and capacity allocation mechanisms in a freeway corridor. *Transportation Research Part C*.2012;(20): 126-143. Available from: doi:10.1016/j.trc.2011.05.005

[21] Papamichail I, Kotsialos A, Margonis I, et al. Coordinated ramp metering for freeway networks – A model-predictive hierarchical control approach. *Transportation Research Part C: Emerging Technologies*. 2010;18(3): 311-331. Available from: doi:10.1016/j.trc.2008.11.002

[22] Carlson RC, Papamichail I, Papageorgiou M, et al. Optimal motorway traffic flow control involving variable speed limits and ramp metering. *Transportation Science*. 2010;44(2): 238-253. Available from: doi:10.1287/trsc.1090.0314

[23] Goatin P, Göttlich S, Kolb O. Speed limit and ramp meter control for traffic flow networks. *Engineering Optimization*. 2016;48(7): 1121-1144. Available from: doi:10.1080/0305215X.2015.1097099

[24] Papamichail I, Kampitaki K, Papageorgiou M, et al. Integrated ramp metering and variable speed limit control of motorway traffic flow. *IFAC Proceedings Volumes*. 2008;41(2): 4084-14089. Available from: doi:10.3182/20080706-5-KR-1001.02384

[25] Carlson RC, Papamichail I, Papageorgiou M, et al. Optimal mainstream traffic flow control of large-scale motorway networks. *Transportation Research Part C: Emerging Technologies*. 2010;18(2): 193-212. Available from: doi:10.1016/j.trc.2009.05.014

[26] Ma M, Liang S. An optimization approach for freeway network coordinated traffic control and route guidance. *PloS one*. 2018;13(9): e0204255. Available from: doi:10.1371/journal.pone.0204255

[27] Ma M, Liang S. An integrated control method based on the priority of ways in a freeway network. *Transactions of the Institute of Measurement and Control*. 2018;40(3): 843-852. Available from: doi:10.1177/0142331216668393

[28] Kotsialos A, Papageorgiou M, Diakaki C, et al. Traffic flow modeling of large-scale motorway networks using the macroscopic modeling tool METANET. *IEEE Transactions on Intelligent Transportation Systems*. 2002;3(4): 282-292. Available from: doi:10.1109/TITS.2002.806804

[29] Sarvi M, Kuwahara M. Using ITS to improve the capacity of freeway merging sections by transferring freight vehicles. *IEEE Transactions on Intelligent Transportation Systems*. 2008;9(4): 580-588. Available from: doi:10.1109/TITS.2008.2006812

[30] Ossenbruggen PJ. Assessing freeway breakdown and recovery: A stochastic model. *Journal of Transportation Engineering*. 2016;142(7): 04016025. Available from: doi:10.1061/(ASCE)TE.1943-5436.0000852

[31] Yu R, Abdel-Aty M. An optimal variable speed limits

system to ameliorate traffic safety risk. *Transportation Research Part C: Emerging Technologies*. 2014;46: 235-246. Available from: doi:10.1016/j.trc.2014.05.016

[32] Zhao S, Liang S, Liu H, et al. CTM based real-time queue length estimation at signalized intersection. *Mathematical Problems in Engineering*. 2015;2015. Available from: doi:10.1155/2015/328712

[33] Ma G, Ma M, Liang S, et al. An improved car-following model accounting for the time-delayed velocity difference and backward looking effect. *Communications in Nonlinear Science and Numerical Simulation*. 2020; 105221. Available from: doi:10.1016/j.cnsns.2020.105221

[34] Liang S, Ma M, et al. Influence of bus stop location upon traffic flow. *Proceedings of the Institution of Civil Engineers-Municipal Engineer*. 2019;04. Available from: doi:10.1680/jmuen.18.00059

[35] Hegyi A, De Schutter B, Hellendoorn H. Model predictive control for optimal coordination of ramp metering and variable speed limits. *Transportation Research Part C: Emerging Technologies*. 2005;13(3): 185-209. Available from: doi:10.1016/j.trc.2004.08.001